IJITCE

ISSN 2347- 3657

International Journal of Information Technology & Computer Engineering

Email : ijitce.editor@gmail.com or editor@ijitce.com

International Journal of Information Technology & Computer Engineering

ISSN 2347–3657

Volume 9, Issue 1, Jan 2021

Emitter detection for the Internet of Things based on transient data using convolutional neural networks and the general linear chirplet transform with optimization

MADHU CHOUHAN

Abstract

In this letter, the General Linear Chirplet Transform (GLCT), a time-frequency representation recently introduced in the literature, is probed for its potential use in conjunction with Using a Convolutional Neural Network (CNN) to recognize IoT wireless devices.

During transmission, radio frequency emissions from the IoT devices are analyzed to determine their identities. By presenting an optimization approach for GLCT tailored to emitter identification, we use the innovative combination of CNN and GLCT (CNN-GLCT) to the transient sections of the radio frequency emissions. We demonstrate empirically that this combination outperforms previous Deep CNN techniques and shallow machine learning methods like SVM and KNN, notably in low Signal-to-Noise Ratio (SNR) and fading environments, where these other methods struggle.

INTRODUCTION

A primary function of security is identification. Authentication may be based on something an entity knows (like a password) or something the entity has (like a smartcard) the entity itself (such as a biometric trait) or something it has created (such as cryptographic material). Multi-factor identification may use two or more of these characteristics simultaneously for positive identification. In this letter, we'll look at one method of identifying electronic gadgets by their unique characteristics; especially, the Radio Frequency (RF) emissions produced by wireless gadgets during transmission. The research literature demonstrates that precise wireless device identification is feasible.

In reality, there are elements in the digitized signal obtained from the RF emissions that are directly connected to the properties of the electronic components, either because of the materials used or the manufacturing process. Multiple publications have shown that this method provides very high identification accuracy over a wide range of protocols, including WiFi [1, 2], the Internet of Things [3, 4], and DSRC [5]. Different terms are used to refer to this method in the specialized literature. Because the inherent traits are conceptually similar to human DNA, it has been given a variety of names, including Radiometric Identification in [5], Special Emitter Identification (SEI) in [6], RF fingerprinting in [7], and RF-DNA in [8].

ASSISTANT PROFESSOR, Mtech,Ph.D
Department of CSE
Gandhi Institute for Technology, Bhubaneswar.

International Journal of Information Technology & Computer Engineering
ISSN 2347–3657
Volume 9, Issue 1, Jan 2021

Special Emitter Identification will be used to describe this method for the remainder of this letter (SEI).

Particularly, we are concerned with the issue of recognizing a wireless device from among a group of wireless devices that all use the same wireless standard (e.g., WiFi). Based on the account given in

According to [9], the following desirable characteristics should be included in any suggested method for this setting: accuracy in a) identification and b) resistance to interference from the wireless propagation medium (e.g., presence of background RF noise or fading).

Recently, Deep Learning (DL) approaches have been employed in comparable scenarios, with considerable improvements in accuracy compared to methods based on hand-crafted features or shallow machine learning algorithms (e.g., [5],[6], and [10]).

What We've Done: In this letter, we discuss the application of CNN plus GLCT (hence referred to as CNNGLCT) to the issue of SEI. Here, we offer a new optimization strategy for choosing the best value for the GLCT algorithm's window parameter. This technique uses the unique properties of SEI to get the best values for such a parameter without carrying out the classification process. As a result, when compared to existing CNN-based classification algorithms, this one dramatically shortens the total processing time. Our empirical findings further demonstrate that, in the presence of Additive White Gaussian Noise (AWGN) and fading effects, CNN-GLCT performs better than other combinations of CNN with time frequency representations seen in the literature. A copy of the dataset used for this reply may be found in IEEE Data Port with the DOI of 10.21227/pqap-7b64.

The paper will proceed as described below. The GLCT and the other time-frequency transformations we evaluate are described in Section II. In Section III, we discuss the system we propose to use to categorize wireless gadgets. The materials of the test bed, the CNN architecture that yielded our findings, the window optimization strategy in GLCT, and the degrading effects (i.e., AWGN and fading) that were utilized to assess the evaluated methods' resilience are all described here. Our experimental findings and associated comparison analyses are presented in Section IV, and a summary and suggestions for further development are provided in Section V.

LINEAR CHIRPLET TRANSFORM IN GENERAL II

The Generalized Linear Chirplet Transform (GLCT) is an innovative Time Frequency (TF) analysis presented in [11].

(LCT). According to [11], GLCT may be used to easily depict multi-component signals that have different non-linear properties. This makes GLCT an excellent tool for implementing SEI-based due to the non-linear nature of transients, which are present in abundance in wireless communication signals. Our experimental findings in Section IV reveal that GLCT is similarly very insensitive to noise. To achieve a high TF resolution, GLCT is a member of the family of parameterized Time Frequency Analysis (TFA) techniques that focus on determining the signal's unique characteristics.

To better depict highly non-linear signals (the transient of the bursts in our example), the first Chirplet Transform (CT) was created in [12] and later improved by various writers. In specifically, in [13] the authors suggested an adaptive TFA approach that uses maximum likelihood estimation to choose the optimal width and chirp rate. All of the aforementioned approaches, as well as other approaches offered in the literature, have limitations when it comes to representing non-linear signals, as detailed in [11]. As such, [11] created the GLCT to remedy these deficiencies. GLCT operates as described below. The typical STFT transform for a signal s(t) is

$$S(t', w) = \int_{-\infty}^{+\infty} w(u - t')s(u)e^{-iwu}du\,, \qquad (1)$$

International Journal of Information Technology & Computer Engineering
ISSN 2347–3657
Volume 9, Issue 1, Jan 2021

where the window used to sever the transmission is denoted by w(ut0).

We need to add a demodulated operator, which is time-variant, to get rid of the modulated element's effect.

Specifically with regards to non-linear signals in this case. This changes Eq. (1) to

$$S(t',w)=\int_{-\infty}^{+\infty} w(u-t')s(u)e^{-iwu}\cdot e^{-ic(t')(u-t')^2/2}du\ ,$$

where $e^{-ic(t')(u-t')^2/2}$ is the demodulated operator.

The signal's Instantaneous Frequency (IF) peaks at its highest value, producing a crisp TF representation, if the demodulated operator is compatible with the modulated element.

having the desired qualities for SEI (such resistance to noise, for example). Identifying such an operator is challenging, particularly for non-linear signals. As an example of a simplification, the conventional LCT may be obtained by approximating the operator using the following equation.;

$$S(t',w,c)=\int_{-\infty}^{+\infty} w(u-t')s(u)e^{-iwu}\cdot e^{-ic(u-t')^2/2}du\ . \tag{2}$$

Even in this reduced form, however, it is not always possible to predict the signal's IF characteristics with certainty (for example, in the presence of many components such as fingerprints).

tool), it is not easy to calculate the value of the expression eic(ut0)2=2.

The authors of [11] suggest introducing a parameter that determines a rotation in the TF plane as a means of defining the GLCT:

$$\alpha=\arctan\left(\frac{2\cdot T_s}{F_s}\cdot c\right)\ . \tag{3}$$

In the above, T_s is the sampling time and F_s is the sampling frequency (10 MHz in our case), as described in Section III-A). Notice that parameter α is between $-\pi/2$ and $+\pi/2$.

Then, Eq. (2) can be rewritten as:

$$S(t',w,\alpha)=\int_{-\infty}^{+\infty} w(u-t')s(u)e^{-iwu}\cdot e^{-it\tan(\alpha)\frac{F_s}{2\cdot T_s}(u-t')^2/2}du \tag{4}$$

If α takes N possible values, the TF plane can be divided into $N+1$ sections through the following expansion:

$$\alpha=-\pi/2+\pi/(N+1),-\pi/2+2\cdot\pi/(N+1),\ldots,-\pi/2+N\cdot\pi/(N+1)\ .$$

Two hyperparameters (arising from the preceding equations) must be experimentally established when employing GLCT to represent the signal in the TF space for SEI. I looked out of the window and saw

and N, the number of values (or chirplets) in the continuation. Improving classification accuracy is our top priority, thus we're focusing on how to best tweak these hyperparameters.

Section IV demonstrates that although parameter N is not very important for maximizing accuracy, the window w does so. However, it might be time-consuming to run CNN-GLCT for all possible values of w in order to optimize w. Here, we offer a hypothesis-based, alternate, and more effective method of optimizing the w parameter based on certain characteristics of SEI. In Section III, we go into depth about this approach.

The Continuous Wavelet Transform (CWT) [5, 14], the Hilbert Huang Transform (HHT) [15], and the Singular Spectrum Analysis (SSA) are all time-frequency domain transforms that are relevant to the topic at hand and are widely used in SEI to encode short, noisy, non-stationary signals such as the transients employed here.

Methodology and Resources III

Contents, Part A: Components

The RF fingerprints have been collected using nine (9) identical Nordic IoT devices. To facilitate a MySensors network, all Nordic IoT gadgets broadcast on the ISM 2.4GHz frequency ranges

ISSN 2347–3657
Volume 9, Issue 1, Jan 2021

used by the industrial, scientific, and medical sectors.

To capture the signal from the Internet of Things, a Software Defined Radio (SDR) N200 receiver from the Universal Software Radio Peripheral (USRP) has been set up with a sample rate Fs of 10 MHz. To ensure consistent data collection, the XCVR2450 front end of the USRP SDR receiver is locked to the GNSS (u-blox NEO6Q GPS receiver) and disciplined to a 10 MHz reference clock. Despite the small sample size, the number of wireless devices we evaluated is comparable to that of the relevant literature (5 devices in [6] and 9 devices in [7]). Since our focus is on the more difficult intra-model classification issue, we additionally emphasize that all nine devices belong to the same model.

Functioning B.

The workflow consists of the following sub-processes.

First, the nine satellites' combined signal in space

An SDR gathers data from wireless Internet of Things devices. Baseband downsampling of the real-valued signal is followed by in-phase and quadrature component (IQ) storage.

Following synchronization and normalizing of the signals (power normalization is achieved by factoring the signal of the collected bursts with their total Root Mean Square (RMS) level), the bursts of traffic corresponding to each payload may be extracted. Then, among all the wireless devices, 800 bursts are chosen, for a grand total of 9800 = 7200. Next, we apply a moving variance to the bursts to isolate the transients displayed in Figure 1, and we use cross-correlation to get them all in sync.

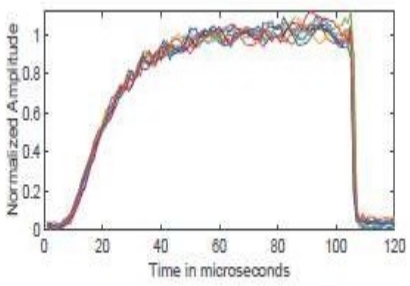

Fig. 1. Transients of the bursts extracted from the IoT emissions. Time is in microseconds (10^{-6} sec.)

The transients are then subjected to a time-frequency transform using the GLCT. The process culminates in a classification evaluation utilizing a Deep Learning CNN classifier and a human judge.

Combinations of CNN and other TF representations, as shown in Section IV, provide results that are inferior to those obtained using deep learning methods.

C. Optimisation of the GLCT

Earlier I indicated that a new optimization technique will be given below in order to compute the w parameter. Because fingerprints are not known in advance, the optimization is predicated on the unique features of the SEI issue. One common technique is optimizing w through a whole CNN time-frequency transformation chain. Instead, we use a time-domain analysis of the signal itself to find the best value for w in our optimization process. From a purely intuitive standpoint, it seems that fingerprints represent a quite sizable departure from the ideal transitory form. Then, using this intuition as a starting point, we conduct an analysis of the standard deviation across transient forms to determine the optimal value for the w parameter that yields the largest standard deviation for all windows of the same width, or width.

$$Opt_w = max(Dev_i^j),\ i = W_1, ..., W_N,\ j = 1, ..., M\ . \quad (5)$$

In the above, Dev_i^j is the value of the standard deviation calculated on the single window j with window size W_i (i.e.,

std(x1:::xWi)) According to the GLCT algorithm and the total size of the transitory SegTran, N is the number of window sizes employed by the method,

ISSN 2347–3657
Volume 9, Issue 1, Jan 2021

and M is the number of iterations through the process.

transitory windows of size Wi (M = SegTran=Wi). The method then repeats the preceding stages for I = W1;::: ;WN, each time calculating the standard deviation for all M windows of size Wi and storing the maximum detected value Devi over all M windows.

The best possible window size, Optw, is found when Devi is maximized. It's important to keep in mind that the method relies on the maximum standard deviation measured on a single window (the one that yields the maximum) for each Wi, rather than on an average of all windows. This is because it is evident that the latter would provide consistent outcomes across all values of Wi. According to Section IV, the findings of this straightforward approach are promising.

The standard deviation calculations are made more accurate in this letter by first adding a smoothing filter to the dataset. These preprocessing processes are exclusively used on the training set in all of our trials.

These methods are referred to as Opt and Opt/Fil, respectively, throughout the remainder of this letter and the subsequent figures.

D. Neural network and machine learning algorithms

From our first studies, we can conclude that the absolute component of the complex signal delivers higher classification accuracy than either the whole complex signal or the phase component alone for all machine learning methods we examined. Limited space prevents us from detailing the outcomes of this comparison here (although comparable conclusions may be found in [5]).

In light of these results, we will focus just on the absolute part of the signal from here on out. The 7200 total samples (800 samples for 9 wireless devices to classify) are divided as follows: a training set of 5400 bursts (of which 1/10, i.e. 540 bursts, is utilized for validation) and a test set of 1800 bursts. A subset of the whole set is randomly selected to serve as both the training and testing sets.

The charts in Section IV show the average value obtained after repeating the categorization procedure 20 times.

As can be seen in Figure 2, the selected CNN network topology is rather complex. Convolutional layer parameters (such as stride) are tuned based on the particular input, whereas the size of the input layer is determined by the timefrequency representation (for example, 80*120 for CNN-CWT). Some kind of padding is applied. The maximum number of pools is 4, and the number of filters may range from 20 to 30. Using a learning rate of 0.001, the RMSProp solver was chosen since it outperformed the competition on this dataset. It turns discovered that this was the optimum form on average across all values of 10i, where I = 2, 3, and 4.

Each batch had 128 iterations, and there were 160 total epochs. To prevent over-fitting, the L2 regularization parameter \swas tuned for each representation (e.g., L2=0.0005 for \sCNN-CWT). To get the best results, this parameter's optimal range was

between one-hundredth of a cent and five cents. When training, the loss function was tuned for Cross-Entropy, and a dropout layer was used.

Here, we put CNN's performance up to that of two "shallow"

The time domain only implementations of the machine learning techniques Support Vector Machine (SVM) using a Radial Basis Function (RBF) kernel, and K Nearest Neighbor (KNN).

Also, the validation set was used to fine-tune the SVM's scaling factor of the RBF kernel and C parameters, as well as the KNN's number of neighbors and distance metrics.

As indicated in Section IV and the following subsections, the test set is subjected to noise and fading conditions.

International Journal of Information Technology & Computer Engineering
ISSN 2347–3657
Volume 9, Issue 1, Jan 2021

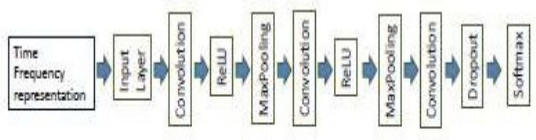

Fig. 2. Schema of the tested CNN architecture.

IV. RESULTS AND ANALYSIS

We optimized the calculation of the window w, as described in Section III-C, and then optimized the value of N independently.

However, our own experiments (not given here owing to space constraints), have demonstrated that increasing N does not noticeably decrease the accuracy of the resultant classifiers. For the following tests, we choose N = 14, which offers a large number of chirplets (from Eq. 4) while keeping the processing time tolerable, in order to strike a suitable compromise between accuracy and processing time. Using the method described in Section III-C, we determined what value window w would have under a range of realistic scenarios (e.g., presence of AWGN and fading effects).

The samples in our training set had a signal-to-noise ratio (SNR) of 50 dB (the baseline data), whereas the samples in our test set had SNRs ranging from -20 dB to 50 dB to mimic the effects of AWGN. This is the typical SNR range cited in the research [5, 10].

In order to account for the effects of fading, the Rayleigh fading model was used; this model uses a fading index Fi between 1 and 10 to parametrize the delay and gain values. In order to calculate the delay vector, we use the following formulae for a four-path channel's delays and gains:

$$delays(sec) = [02 * F_i, 6 * F_i] * 10^{-6}$$
$$gains(dB) = [0, -F_i, -(F_i * 2), -(F_i * 3)] .$$

The fading effects become more significant with lower Fi values, leading to a corresponding drop in classification accuracy. Both the training set and the testing set were produced with Fi=10 to maximize the likelihood of success.

Different choices of w are used to evaluate our optimization strategy (with and without filter) against the gold standard. In Section IV-A and IV-B, we detail these findings.

A. Comparison to other techniques in the presence of AWGN

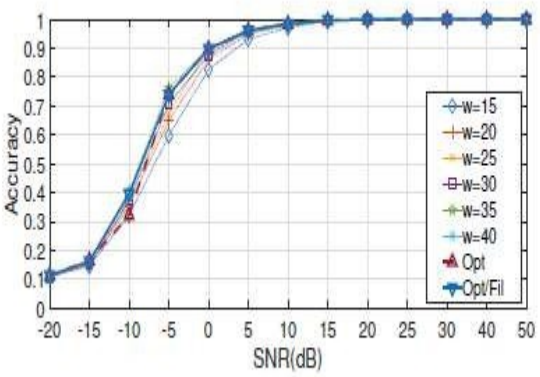

Fig. 3. Accuracy against SNR in dB, at different values of the window size *w* with *N*=14.

In this part, we provide the empirical findings of a comparison between CNNGLCT and three other CNN combinations (CNN-SSA, CNN-CWT, and CNN-HHT) and the time domain alone.

Interpretation CNN-T rated at [10]. Classification algorithms based on support vector machines and k-nearest neighbors when applied to the time domain (SVM-T and KNN-T, respectively) serve as a benchmark for comparison in this study [2].

We started by testing how well our GLCT optimization strategy worked when AWGN was present. As shown in Figure 3, the Opt/Fil method successfully determines the best window widths for a broad range of SNR values in decibels. For specific levels of SNR (for example, SNR=-10db), the Opt method performs marginally worse than Opt/Fil, indicating that the use of the filter is advantageous to the optimization procedure.

International Journal of Information Technology & Computer Engineering
ISSN 2347–3657
Volume 9, Issue 1, Jan 2021

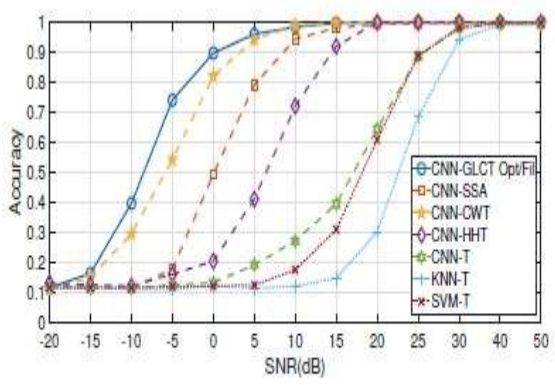

Fig. 4. Comparison of the classification accuracy at different values of SNR using CNN in combination with different time frequency representations and the time domain representation with CNN, SVM and KNN.

You can see how CNN-GLCT stacks up against the competition in Figure 4. Based on these results, we may conclude the following.

The usual combination of time domain and CNN, commonly employed in the literature (e.g., [10]), is considerably outperformed by Time Frequency representations paired with CNN;

b) When compared to the various TF representations we tried, including SSA, HHT (by a large margin), and CWT, GLCT performed the best (used in combination with CNN in [5]).

The TF representations seem to be especially resilient to AWGN, with CNN-GLCT Opt/Fil attaining the highest performance, although all the offered approaches may yield a very high classification accuracy for large levels of SNR.

The impact of fading on B. A comparison to different ways

In this article, we discuss the results of our trials testing resistance to fading (Figure 5 and Figure 6). Optimized methods are compared to the gold standard initially (Figure 5). As opposed to the AWGN scenario, the Optimized methods only perform optimally under mildly degraded fading circumstances (i.e., Fi > 3). Similar to AWGN, Opt/Fil yields superior outcomes than Opt (e.g., Fi > 5). However, the method does not provide ideal outcomes in the presence of severe fading (Fi 3)..

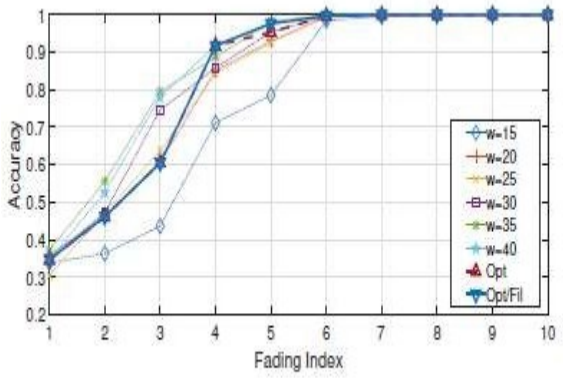

Fig. 5. Comparison of the classification accuracy for different values of parameter w using CNN-GLCT in the presence of fading.

Figure 6 shows that our findings with AGWN are supported by a comparison to the other baselines using CNN-GLCT.

Despite using a predetermined value of w, CNN-GLCT still produces good results.

superior accuracy as compared to alternative baselines for the vast majority of fading index Fi values. CNN-CWT and CNN-HHT outperform CNN-GLCT only in very severe fading (Fi = 1). On top of that, time frequency representations are far more effective than shallow machine learning methods when dealing with fading.

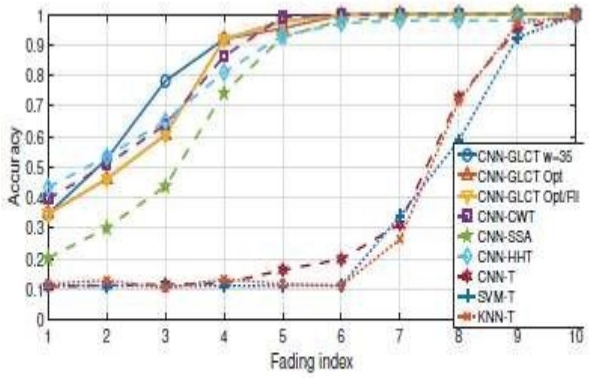

Fig. 6. Comparison of the classification accuracy at different values of the fading index F_i using CNN with different time frequency representations and the time domain representation with CNN, SVM and KNN.

V. CONCLUSIONS

We've looked at using GLCT in conjunction with CNN to identify IoT wireless devices based on the fluctuations in their bursts. The Outcomes demonstrate that compared to the time domain representation of the signal or the CWT and SSA

ISSN 2347–3657
Volume 9, Issue 1, Jan 2021

representations, GLCT gives superior identification accuracy, particularly in the presence of AWGN and fading effects. We also suggested a more ad hoc method for finding the best possible GLCT window size. The results show that this works very well in the AWGN case and works reasonably well in the fading situation. To further explore the method provided here, GLCT will be applied to more emitter identification datasets in the future.

REFERENCES

[1] D. R. Reising, M. A. Temple, and J. A. Jackson, "Authorized and rogue device discrimination using dimensionally reduced RF-DNA fingerprints," IEEE Transactions on Information Forensics and Security, vol. 10, no. 6, pp. 1180–1192, June 2015.

[2] V. Brik, S. Banerjee, M. Gruteser, and S. Oh, "Wireless device identification with radiometric signatures," in Proceedings of the 14th ACM international conference on Mobile computing and networking. ACM, 2008, pp. 116–127.

[3] G. Baldini, R. Giuliani, and F. Dimc, "Physical layer authentication of internet of things wireless devices using convolutional neural networks and recurrence plots," Internet Technology Letters, vol. 2, no. 2, p. e81, 2019.

[4] G. Baldini, G. Steri, R. Giuliani, and F. Dimc, "Radiometric identification using variational mode decomposition," Computers & Electrical Engineering, vol. 76, pp. 364–378, 2019.

[5] G. Baldini, C. Gentile, R. Giuliani, and G. Steri, "Comparison of techniques for radiometric identification based on deep convolutional neural networks," Electronics Letters, vol. 55, no. 2, pp. 90–92, 2018.

[6] L. Ding, S. Wang, F. Wang, and W. Zhang, "Specific emitter identification via convolutional neural networks," IEEE Communications Letters, vol. 22, no. 12, pp. 2591–2594, 2018.

[7] K. Yang, J. Kang, J. Jang, and H.-N. Lee, "Multimodal sparse representation-based classification scheme for RF fingerprinting," IEEE Communications Letters, vol. 23, no. 5, pp. 867–870, 2019.

[8] D. R. Reising, M. A. Temple, and M. E. Oxley, "Gabor-based RF-DNA fingerprinting for classifying 802.16 e wimax mobile subscribers," in

Computing, Networking and Communications (ICNC), 2012 International Conference on. IEEE, 2012, pp. 7–13.

[9] Q. Xu, R. Zheng, W. Saad, and Z. Han, "Device fingerprinting in wireless networks: Challenges and opportunities," IEEE Communications Surveys Tutorials, vol. 18, no. 1, pp. 94–104, Firstquarter 2016.

[10] K. Merchant, S. Revay, G. Stantchev, and B. Nousain, "Deep learning for RF device fingerprinting in cognitive communication networks," IEEE Journal of Selected Topics in Signal Processing, vol. 12, no. 1, pp. 160– 167, 2018.

[11] G. Yu and Y. Zhou, "General linear chirplet transform," Mechanical Systems and Signal Processing, vol. 70-71, pp. 958 – 973, 2016. [Online]. Available: http://www.sciencedirect.com/science/article/pii/S0888327015003994

[12] S. Mann and S. Haykin, "The chirplet transform: physical considerations," IEEE Transactions on Signal Processing, vol. 43, no. 11, pp. 2745–2761, Nov 1995.

[13] H. K. Kwok and D. L. Jones, "Improved instantaneous frequency estimation using an adaptive short-time fourier transform," IEEE Transactions on Signal Processing, vol. 48, no. 10, pp. 2964–2972, Oct 2000.

[14] J. Zhang, F. Wang, O. A. Dobre, and Z. Zhong, "Specific emitter identification via hilbert–huang transform in single-hop and relaying scenarios," IEEE Transactions on Information Forensics and Security, vol. 11, no. 6, pp. 1192–1205, 2016.

[15] R. Vautard, P. Yiou, and M. Ghil, "Singular-spectrum analysis: A toolkit for short, noisy chaotic signals," Physica D: Nonlinear Phenomena, vol. 58, no. 1-4, pp. 95–126, 1992.